

Novel Strategy for Three-Dimensional Fragment-Based Lead Discovery

Haoliang Yuan, Tao Lu, Ting Ran, Haichun Liu, Shuai Lu, Wenting Tai, Ying Leng, Weiwei Zhang, Jian Wang, and Yadong Chen*

Laboratory of Molecular Design and Drug Discovery, School of Basic Science, China Pharmaceutical University, 24 Tongjiaxiang, Nanjing 210009, China.

ABSTRACT: Fragment-based drug design (FBDD) is considered a promising approach in lead discovery. However, for a practical application of this approach, problems remain to be solved. Hence, a novel practical strategy for three-dimensional lead discovery is presented in this work. Diverse fragments with spatial positions and orientations retained in separately adjacent regions were generated by deconstructing well-aligned known inhibitors in the same target active site. These three-dimensional fragments retained their original binding modes in the process of new molecule construction by fragment linking and merging. Root-mean-square deviation (rmsd) values were used to evaluate the conformational changes of the component fragments in the final compounds and to identify the potential leads as the main criteria. Furthermore, the successful validation of our strategy is presented on the basis of two relevant tumor targets (CDK2 and c-Met), demonstrating the potential of our strategy to facilitate lead discovery against some drug targets.

1. INTRODUCTION

Recent years have seen a tremendous increase in novel drug discovery technologies. Fragment-based drug design (FBDD) has emerged as an important methodology for the generation of high-quality leads.^{1–4} FBDD adopts a constructive strategy that affinity is enhanced by cycles of adding functional groups or linking two independent fragments together. Primarily, FBDD requires various low-molecular-weight chemical fragments that bind in adjacent regions of the target active site. The exact binding modes of these fragments can provide some spatial structural information to guide fragment optimization. Once bound to the active site of a target protein, the fragments can be developed into highly selective and potent drug candidates, particularly when their binding mode to the target protein has been determined by three-dimensional structural elucidation through nuclear magnetic resonance (NMR) spectroscopy or X-ray crystallography. The observed fragments bind in relatively close proximity to one another, providing data with which the different functionalities can be linked or merged, within a single, ideally potent ligand. One of the foundational principles of FBDD is that, upon modification, the initial fragment lead maintains its original orientation in the protein-binding pocket and, thus, contributes to the final binding energy. Therefore, the final inhibitor is expected to adopt the same geometry as the original fragment hit.⁵ However, this intriguing concept resulted in only a few applications and had no immediate impact on drug discovery,^{5–7} and problems remain to be solved to put this strategy into practice.

For FBDD, the most crucial stage is to identify the high-quality fragments. The fragments must be unambiguously and experimentally detected to characterize the binding of their weak interactions with the target. The availability of the experimental structural information of the fragments bound to their target promotes the progression from relatively simple, minimally functionalized, weak hits to potent, elaborated leads. However, the

small sizes of the fragments make them difficult to screen. Classical biophysical assays are generally incapable of detecting fragments with low binding affinity.^{8,9} It is more difficult to identify fragments that simultaneously bind to adjacent regions of the target binding site. Moreover, a report has shown that analogues of fragment hits are more likely to adopt alternate binding modes.¹⁰

Alternatively, prior knowledge on where specific chemical fragments bind to a protein can be used in a broad range of computational techniques.^{11,12} A variety of computational tools have been developed for identifying fragments. However, the prediction of binding modes for fragments using computational methods remains problematic. Fragments generally have fewer internal degrees of freedom than larger compounds, and their location and orientation within a binding pocket can be more difficult to predict because alternative binding is more likely to yield similar scores or predicted binding energies. Computations of free energies and binding modes by docking experiments are not yet sufficiently accurate to help discover fragments. Thus, a more efficient approach to the discovery of fragments and potent leads for drug design is needed.

Currently, an increasing number of drug candidates have been determined in a complex with the same target by crystallography. The abundant structural information obtained from cocrystallized target proteins and their various inhibitors can effectively facilitate fragment-based lead discovery. Herein, we propose a computational strategy for deconstructing aligned drug candidates bound to the same target protein and converting their cocrystallized or docking conformations into fragments. Such fragments maintain their original binding modes and spatial orientations at the same active site. Thus, after linking or merging the fragments bound in different regions of the active site, a novel

Received: January 5, 2011

Published: March 25, 2011

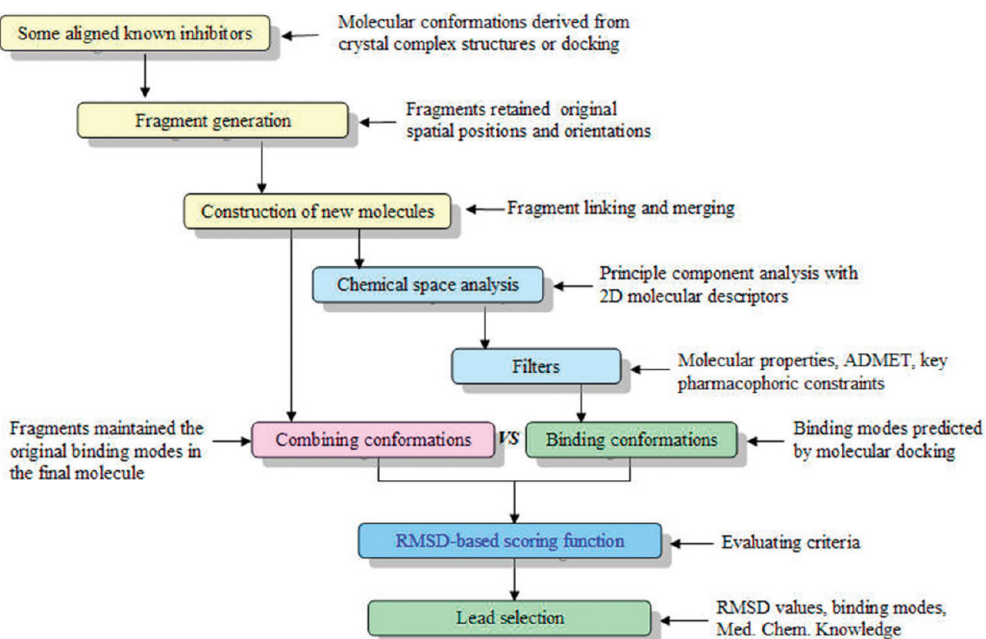


Figure 1. Workflow schematic for the novel lead discovery strategy.

ligand with a substantially improved affinity for the target could be generated. This method might prove to be extremely rapid and efficient in producing very active molecules. In this strategy, we focus on solving two problems. First, we sought to obtain suitable fragments that bind simultaneously to separate regions of the binding sites, and second, we combined these fragments without significant changes in their initial binding modes. Furthermore, we evaluated our lead generation strategies with two case studies using cyclin-dependent kinase 2 (CDK2) and c-Met.

2. MATERIALS AND METHODS

2.1. Overview of the Present Strategy. An overview of our strategy is schematically described in Figure 1. First, known structurally diverse inhibitors with cocrystallized or docking conformations in the same protein target were superimposed and then deconstructed into small fragments according to predefined fragmentation rules. The fragments that bound to adjacent sites of the target protein were then linked or merged to create the desired, novel molecules. The new molecules were not subjected to energy minimization. At this time, the conformation of the new molecule maintained the original binding modes of the fragments, which is called combining conformation. A variety of methods were then used to analyze and filter the new molecular library to obtain the molecules that matched the basic properties and key pharmacophoric constraints. The root-mean-square deviation (rmsd) values between the combining and docking conformations of the new molecules were calculated. The rmsd-based scoring function was used as the main criterion for lead selection. The details of each step are described in the subsequent sections.

2.2. Initial Inhibitor Set Preparation. To obtain suitable fragments that bind to the adjacent binding sites, known inhibitors bound to the active site of the same target protein were used to generate fragments. The initial representative known inhibitors against the same target were selected from published results according to their chemical diversity. The inhibitors within the

crystal complex structures were superimposed onto the reference crystal structure using the default parameter settings of the protein structure alignment software. Without the experimentally resolved structures of the inhibitors within the complex of the target protein, accurate molecular docking simulations were performed to obtain their binding conformations. Therefore, the binding conformations of these known inhibitors were well-aligned in the same active site and then extracted from the complex structures to generate three-dimensional fragments.

2.3. Three-Dimensional Fragment Generation. Suitable fragments located in adjacent regions of the same active site were obtained by deconstructing the aligned inhibitors with their binding conformations based on some simple rules, similar to those described in the original report on the retrosynthetic combinatorial analysis procedure (RECAP).¹³ According to this approach, hydrogen bonds and ring-connecting bonds are never cleaved, and molecules with more than the defined “maximum atoms” (i.e., maximum number of atoms allowed in the molecule to be fragmented) are not cleaved. The minimum number of non-hydrogen atoms in a fragment was set to 2. It is an option to set whether the bonds between carbons and heteroatoms should be cut. The retrieved fragments are denoted, for example, 1oiq_fragment1, where 1oiq is the PDB code of the initial inhibitor and fragment1 is the serial number of the generated fragment. All resultant fragments in the library are not only suitable for separate regions of the active site, but also maintain their original binding modes and conformations of the initial known inhibitors within the protein target active site.

2.4. Construction of New Molecules. The construction of new molecules is performed automatically by linking or merging the spatial neighboring fragments through a set of bonding rules. Some constraints, such as angle deviation and distance, are set to prevent spatial conflicts. The fragments are joined after the bonds that can be formed between the fragments have been identified. The bonds are identified by two criteria: (1) the angle between the bond directions must be less than a threshold (default is 15°), and (2) the distance between the atom that remains in one

fragment and the atom that leaves the other fragment must be less than a threshold (i.e., after the bond lengths have been adjusted to the ideal bond length; default is 1 Å). The former criterion ensures the proper rotational alignment of the fragments, and the latter ensures the proper translational alignment of the fragments.

Both internal and peripheral (i.e., H and halogen) bonds can be considered for breaking to form a bond with another fragment, and the fragments can overlap. However, if the distance between the fragment centroids is below the given threshold of 3.0 Å, then the fragments cannot join because they are considered to occupy the same location in the receptor. The self-assembly of fragments is accomplished after several rounds. The first round joins pairs of fragments. In the second round, the results of the first round are used as input, so that the generated molecules can be combinations of up to four fragments, and so on. Four rounds were performed so that new molecules could be made with the resultant molecules from the previous round.

The new molecules are not allowed to be constructed with the fragments from the same initial inhibitor to ensure the novelty of the new compounds, judging from the fragment names. Methylene linkers are included to assess whether a bond can be formed for fragments that do not contain atoms that are close enough to create new bonds and are still not far apart. One methylene group is added to each fragment; thus, two fragments can be linked with at most two methylene linkers. Fragment merging is performed if the carbon–hydrogen or carbon–halogen bonds in the different fragments bound in adjacent regions of the active pocket overlap.

A whole molecule obtained by combining (linking or merging) adjacent fragments is generally subjected to energy minimization. However, the energy minimization procedure is not performed in this strategy, so that the constituent fragments of the final compounds will maintain their original conformations in separate regions of the active site.

2.5. Evaluation of Constructed Molecular Library. To finally find promising leads, several methods were applied in evaluating the quality of the new molecular library, including chemical space analyses, molecular docking, pharmacophoric constraints, and rmsd calculations.

2.5.1. Analysis of Molecular Libraries. Chemical space can be maximally probed in FBDD.¹⁴ In this strategy, only certain representative inhibitors are selected from all categories. The chemical space coverage of the initial known inhibitors and the newly constructed fragment-based molecular library are compared to ensure that the chemical space is maximally probed. The chemical diversity should be at least as broad as that of the initial inhibitor set to demonstrate the novelty of the new molecular library. To present the relationship of the covered chemical space in a meaningful and accessible way, it is useful to construct graphical distributions of the data set in three-dimensional space. Mapping chemical space using molecular descriptors has been successfully applied to describe the medicinal chemistry space and express the shared chemical space covered with inhibitors against different targets.^{15,16} Thus, we applied this method to determine the coverage rate comparison.

Two-dimensional descriptors, which describe the atomic nature, molecular size, polarity, lipophilicity, and flexibility, are first calculated using the Molecular Operating Environment (MOE) software package. Principal-component analysis (PCA) is a relatively easy way to transform an *n*-descriptor space into a more-manageable three-dimensional space. In our analysis, the 39-vector space was transformed into a three-dimensional space

described by three principal component vectors, where each of the three vectors is a combination of 39 weighted descriptors.¹⁷ These operations facilitate the creation of graphical representations of the three-dimensional space spanned by the compound sets. From this three-dimensional graphic, it is easy to evaluate whether the chemical space could be maximally probed.

2.5.2. Compound Filtering. To discard the new molecules with unfavorable properties, several types of filters are applied. Lipinski's "rule of 5" is the first criterion used to evaluate the promising "drug-like" properties of the new molecular library, which concerns orally active compounds, by defining four simple physicochemical parameter ranges: molecular weight ≤ 500, log *P* ≤ 5, H-bond donors ≤ 5, and H-bond acceptors ≤ 10.¹⁸ Other criteria can be added if the specific properties, such as ADMET (absorption, distribution, metabolism, elimination, toxicity) constraints, are required. The new molecular library is subjected to this filtration through a workflow protocol constructed in the pipeline pilot software package.

Structure-Based Key Pharmacophore Constraints. Small contributions from the molecular fragments match various pharmacophoric features in the different active site binding regions and can be combined to yield a high-affinity ligand. Diverse ligands are selected to generate fragments, which are located in adjacent regions of the active site and contribute strongly to the final protein–ligand binding interaction. It is beneficial for the interactions between the binding pocket and the new molecules if the latter are constructed with fragments located in different regions, especially those having critical interactions with the active site. A structure-based pharmacophore model was developed with Accelrys Discovery Studio 2.5 according to the analyzed protein–ligand binding interactions. The key pharmacophoric features were used as constraints in the new molecular library filtration to obtain molecules containing crucial fragments for their interaction with separate regions of the binding pocket.

Molecular Docking. Molecular docking is applied to prioritize the new molecular library and obtain the binding conformations of the new molecules in the active site. Glide has shown good reproducibility of cocrystallized ligand conformations, which has also been recommended in some literature reports because of its accuracy in molecular docking and scoring.¹⁹ Therefore, it was selected as the molecular docking tool. The crystallized complex structure selected was prepared with the Protein Preparation Wizard workflow. The generated receptor grid is centered on the cocrystallized ligand, which is defined as the ligand-binding site search region. The ligand to be docked is confirmed by an enclosing box that is similar in size to the cocrystallized ligand. The compound set for docking is prepared with the LigPre module. The best conformation of each compound comprises the output on the basis of the Glide score and interactions formed between the ligands and active site. Default settings are kept for all remaining parameters. The potential compounds are then flexibly docked into the binding site with the extra precision (XP) docking mode selected.

2.5.3. rmsd-Based Scoring Function. The generated combining conformations of the new molecules maintain the original binding modes of their component fragments because no energy minimization is applied in the fragment combining process. Docking is used to predict the binding conformations of the new molecules with their protein targets. To investigate whether the component fragments in the final molecules maintain their original binding modes, the rmsd between the docking and combining conformations is applied as a criterion to evaluate the distortions of the component fragment binding modes.

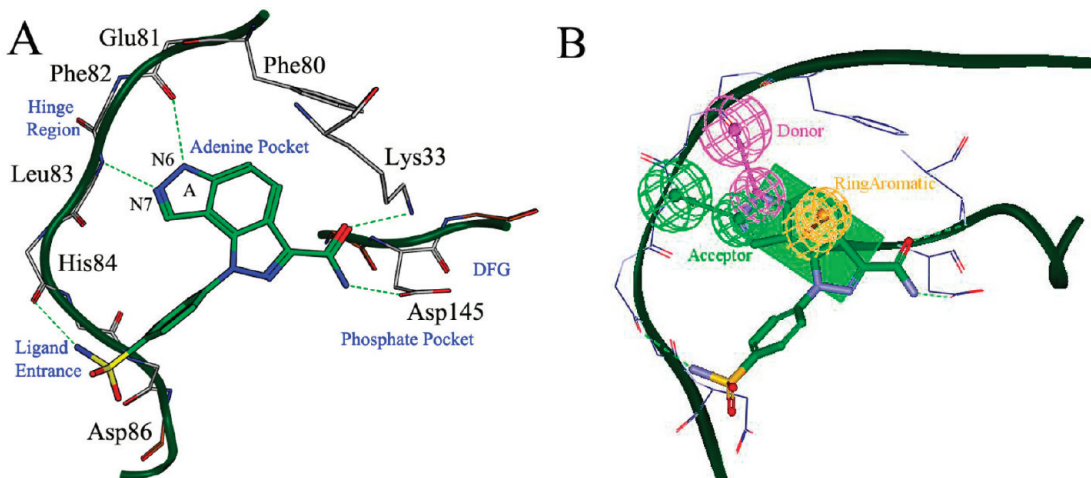


Figure 2. (A) Interactions between inhibitor 27 and the ATP-binding pocket. (B) Three key pharmacophoric features of CDK2 inhibitors: donor, acceptor, and aromatic ring.

The two conformation types are imported into the Match Atoms module within Sybyl to align the different conformations or locations of the same molecules. The Match module performs a search of all possible matches based on connectivity. The rmsd values are calculated between the corresponding non-hydrogen atoms, and all hydrogen atoms are excluded from the matching process.

3. RESULTS AND DISCUSSION

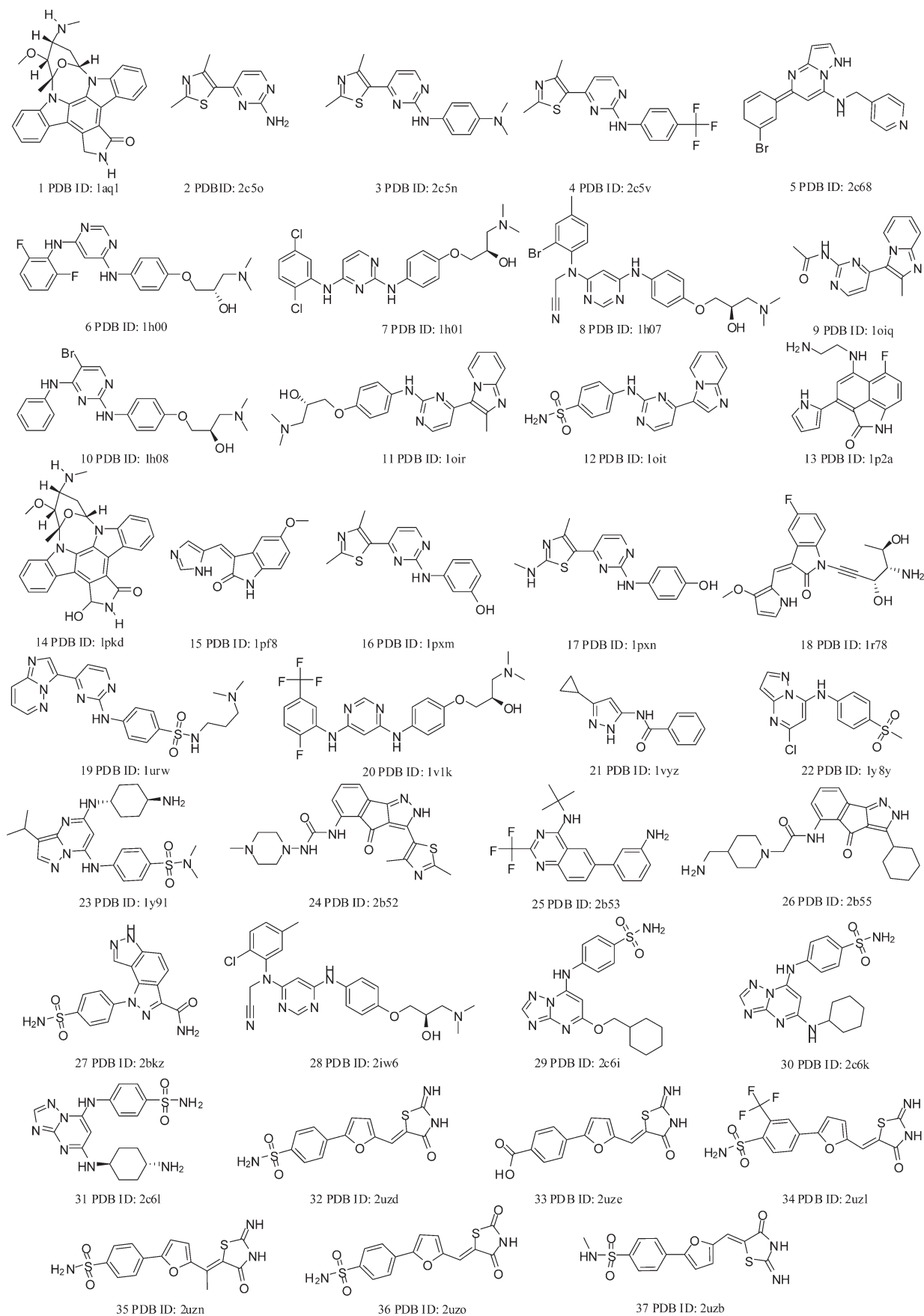
3.1. Fragment-Based Lead Discovery Strategy. *3.1.1. Three-Dimensional Fragment Generation.* Fragments can be obtained through experimental detection or computational methods. However, in the process of fragment library generation, many limitations exist for both methods. The fragments that pass through a bioactivity assay are selected for binding mode detection. However, it is difficult to obtain suitable fragments in the adjacent regions of the same active site through binding mode detection because of their low affinities. Additionally, high economic and time costs are barriers for the practicality of these methods in common groups.¹⁴ Computational approaches are the best alternative for experimental FBDD. Generally, the fragments are generated using a prefiltered commercial fragment database. The compounds are then docked into the binding pocket to obtain their binding conformations, and then conformational scoring is performed to select suitable fragments for consequent studies. However, current, prevalent docking tools are inefficient for simulating fragment binding because the fragments are much smaller than common compounds, making it difficult to fully take their flexibility into account in a comparably large binding pocket. False positives can also result. Most scoring functions have been developed to reproduce the binding energies of drug-like compounds, which exhibit much higher affinities for binding than do fragments. The scoring and ranking of the fragments, which have lower affinities for the binding site, can be more difficult because the development of reliable scoring schemes of drug-like molecules is still a challenge.²⁰

Although some leads have been found with experimental fragment-based methods,²¹ problems regarding fragment binding conservation have also been observed. Babaoglu and Shoichet showed that component fragments could not recapitulate the

binding geometry of larger and higher-affinity inhibitors when deconstructed into three small fragments. The three component fragments bound to the previously unexplored binding sites at the surface of the protein.²² Consistent with this case, Barelier et al. reported that component fragments will interact with their preferred binding site, which could be different from the site they occupied when they were parts of a larger molecule.²³ However, in principle, the ideal lead compounds should be molecules that are made up of smaller fragments and linked together to retain the same position and orientation on the protein whenever they are separate or sections of larger lead compounds.²⁴ Inconsistencies have been found between the fundamental principle and the experimental studies described above. Therefore, computational fragment-based approaches present the best alternative to experimental methods in solving fragment binding conservation problems.

We present this novel strategy to align inhibitors well against their same target to generate a fragment library. The complexed structures are obtained from the protein–ligand cocrystal structures or by molecular docking after being superimposed onto the reference. The three-dimensional binding conformations of the ligands extracted from these complexed structures are then used for rigid fragment generation following certain rules. There are significant differences between our strategy and other methods. The known inhibitors in the initial set are selected according to their structural diversity and bioactivity. Different regions of the active site can be fully probed because structurally diverse, known inhibitors with good bioactivities have occupied almost all regions in the active site. Suitable fragments are rigidly obtained in almost all binding regions to avoid difficulties that include the simultaneous identification of potent fragments binding in adjacent regions of the active site by experimental methods. In addition, without any artificial modifications, the generated component fragments will maintain their original spatial positions and orientations. In consequence, the fragment binding conformations are more accurate than those predicted with fragment docking. Although some complex structures are obtained with molecular docking, it is more accurate and easier to predict the binding conformations of whole molecules than fragments with computational methods. Fewer fragments might be obtained with this strategy, and even duplicates with the same

Chart 1. Two-Dimensional Chemical Structures of Initial 37 Known Inhibitors That Were Cocrystallized with CDK2



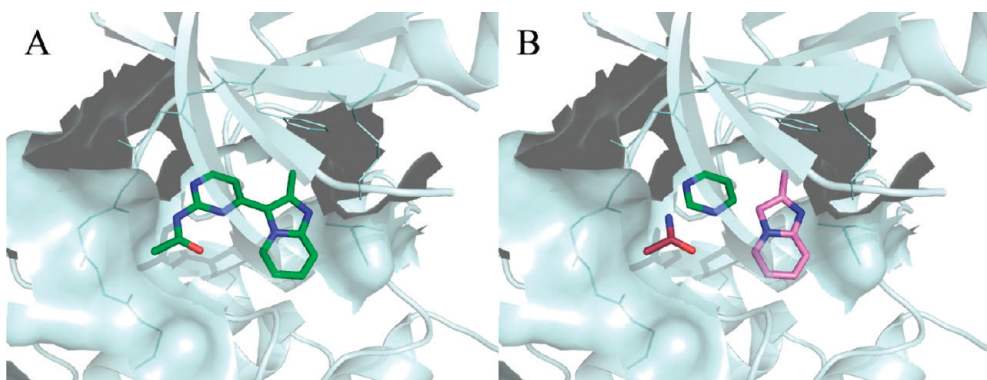


Figure 3. (A) Binding conformation of inhibitor 9 (PDB ID 1OIQ). (B) Conformations of the three component fragments deconstructed from inhibitor 9: fragment 1 (red), fragment 2 (light green), and fragment 3 (pink).

chemical structures might exist in the fragment library. However, different spatial positions and orientations of these fragments within the active site keep them in the fragment library. Furthermore, costs are significantly reduced without the use of various experimental methods to detect fragment conformations.

Compound deconstruction rules are also very important in fragment library generation. RECAP¹³ is a classical method that includes 11 fragmentation rules based on retrosynthetic chemistry knowledge. These rules are similar to those described in the original RECAP article.¹³ However, the three-dimensional binding information is retained when the known inhibitors are deconstructed into fragments. Therefore, we present this novel computational strategy to deconstruct the known inhibitors while complexed with their target protein, cocrystal complex structures, or predicted computational structures, into fragments bound to the active site of a target protein.

3.1.2. Construction and Evaluation of New Molecular Library. An active inhibitor is usually developed through fragment growth or linking. For fragment growing, functional groups are added to the initial detected fragments, guided by fragment binding orientation. The binding conformations of the final compounds are then analyzed using NMR spectroscopy, X-ray crystallography, and other methods to validate the hypotheses about spatial position. Depending on their binding mode and synthetic tractability, some of the fragments might not be suitable for use as starting points. Before the fragment linking approach can be initiated, the fragment binding in a region adjacent to the first one should be identified. Although many techniques have been reported to screen a second fragment site in the presence of a known fragment²⁵ and identify a pair of ligands that bind simultaneously in a single fragment mixture,²⁶ it is still difficult for common research groups to apply these techniques in daily studies. Additionally, fragment linking is also very sensitive to linker design, which should not perturb the binding mode of the detected fragments.²⁷ Studies have shown how little the initial fragments move because fragments are prone to take different positions after fragment linking.²⁸ Thus, how the detected potential fragments can be linked without distorting their individual binding modes is also one of the problems for practical applications of FBDD.²⁹

Given the problems described above, an alternative method for fragment-to-lead applications is presented with this novel strategy. Fragments binding in the proximal regions in the active site are obtained by deconstructing the known inhibitors, which might be beneficial for improving the feasible syntheses of the new

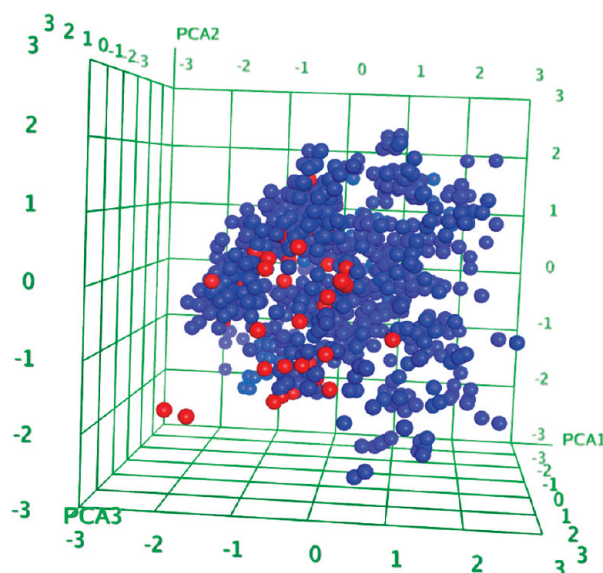


Figure 4. Chemical space covered by the initial 37 inhibitors (red balls) and the constructed molecular library (blue balls).

molecules. Fragment merging is performed if the carbon–hydrogen or –halogen bonds of the different fragments binding in adjacent regions overlap. For fragments that contain no atoms that are close enough to create new bonds but are still not far apart, methylene linkers (at most two) are added to link the proximal fragments and form an entire drug-like molecule. With their combining conformations, the new molecular library is obtained after the fragment-to-lead progression is completed. The final resultant molecules generally pass through an energy minimization procedure to obtain their preferred conformation. However, the purpose is to explore whether the fragment conformations will be affected after their construction into whole molecules. Thus, the molecules in the library are obtained without energy minimization to preserve the component fragment original conformations. These combining conformations might be different from those of the new molecules.

In FBDD, efficiently screening the molecular library to find potential molecules is also an important issue. A filtering protocol, including a series of methods, is applied in this strategy. New molecules are constructed with fragments that bind to different regions of the active site. Those constructed without fragments

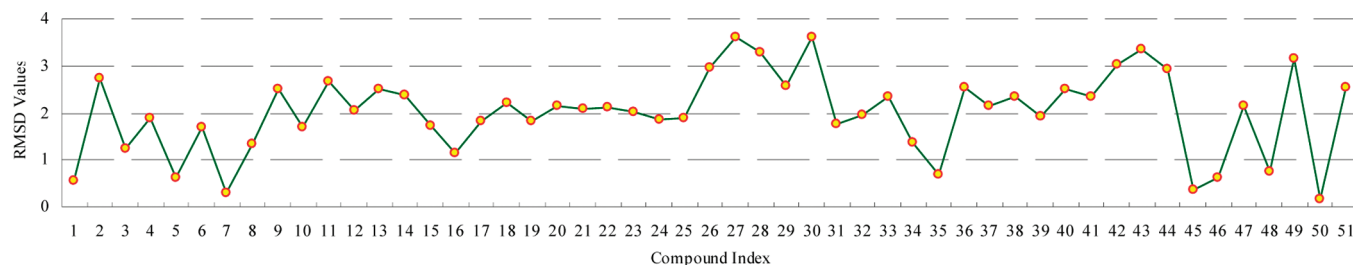


Figure 5. rmsd value distribution of the 51 potential compounds against CDK2.

Table 1. Ranking of the 51 Potentially Active Compounds Using the rmsd Values

ranking	name	index	rmsd	cluster	ranking	name	index	rmsd	cluster
1 ^a	compound 985	48	0.178557	1	27	compound 2765	22	2.125654	1
2	compound 2539	7	0.296109	1	28	compound 2756	20	2.142787	3
3 ^a	compound 561	50	0.355385	2	29	compound 4001	37	2.14287	1
4 ^a	compound 1047	1	0.56003	1	30	compound 695	45	2.161025	1
5 ^a	compound 67	51	0.607436	3	31	compound 2748	18	2.201639	3
6 ^a	compound 2030	5	0.615974	2	32	compound 4203	41	2.334673	1
7	compound 3842	35	0.696241	1	33	compound 3791	33	2.335611	3
8	compound 712	46	0.736847	1	34	compound 4004	38	2.338516	3
9	compound 2626	16	1.125422	1	35	compound 2607	14	2.379866	3
10 ^b	compound 1250	3	1.242246	3	36	compound 2606	13	2.494324	3
11	compound 2540	8	1.34553	1	37	compound 2594	9	2.502684	3
12	compound 3840	34	1.380409	1	38	compound 4066	40	2.509209	3
13	compound 2537	6	1.680742	1	39	compound 991	49	2.534841	1
14	compound 2600	10	1.696002	1	40	compound 3843	36	2.544564	3
15	compound 2620	15	1.713484	1	41	compound 3320	29	2.579069	1
16	compound 3692	31	1.763615	1	42	compound 2604	11	2.669516	3
17	compound 2750	19	1.822397	3	43	compound 1153	2	2.728509	2
18	compound 2735	17	1.824774	3	44	compound 5510	44	2.919786	2
19	compound 2806	24	1.8463	1	45	compound 2991	26	2.962711	2
20	compound 1271	4	1.874238	2	46	compound 4866	42	3.029405	2
21	compound 2843	25	1.899037	1	47	compound 8769	47	3.160949	1
22	compound 4063	39	1.927048	1	48	compound 3266	28	3.276536	3
23	compound 3788	32	1.948171	1	49	compound 4922	43	3.341717	2
24	compound 2781	23	2.00675	2	50	compound 3133	27	3.606485	2
25	compound 2605	12	2.055486	3	51	compound 3333	30	3.619821	1
26	compound 2758	21	2.080523	3					

^a Compounds belonging to external known inhibitors, not including in the initial CDK2 inhibitor set. ^b Compounds belonging to the initial CDK2 inhibitor set.

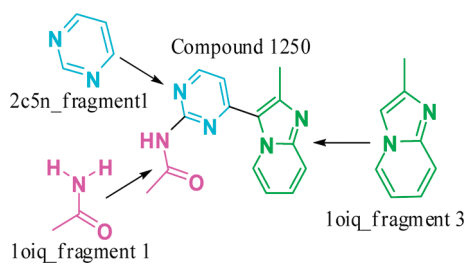
that bind to the key regions are considered to be less potential inhibitors. Therefore, key pharmacophoric features are first used as constraints to filter the new molecular library and ensure that the compounds interact with the critical regions of the active pocket and that all are retained. The scoring functions implemented in the molecular docking program are also used to rank the new molecules. Problems, such as false positives and false negatives, usually occur during molecular docking methods, and it is not reliable enough to assess these molecules only according to this program. Consequently, a more accurate scoring function with higher compatibility with this FBDD strategy is necessary.

In this strategy, fragments are obtained after deconstructing selected known inhibitors within their active conformations,

maintaining their best conformation for interacting with the residues in the active site. The final molecule is expected to adopt the same binding geometry as the original component fragments in the active site. Therefore, the deviation between the combining and binding conformations should be investigated to determine whether the fragments maintain the original binding modes in the final molecules. The rmsd values reflecting the difference between the combining and binding conformations are applied as the scoring functions to assess the new molecular library. The compounds with lower rmsd values are considered as high potential active inhibitors. Only those new molecules with rmsd values below a certain threshold (3 Å) are accepted, which indicates that the component fragments are combined without significant changes of their individual binding modes in the final

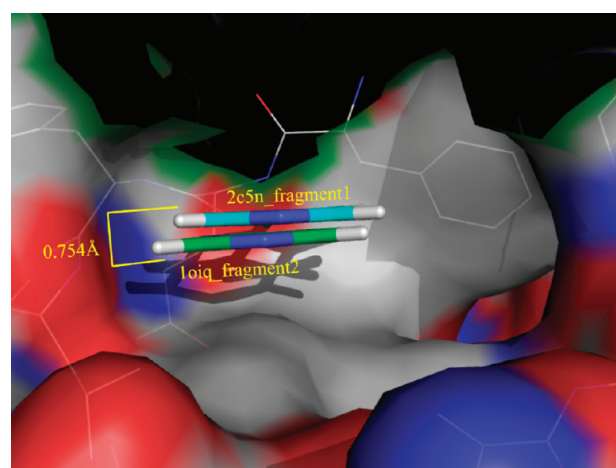
Table 2. Six Known CDK2 Inhibitors Generated by This Strategy

Comp. No.	Structures	RMSD	Fragment1 (Green)	Fragment2 (Blue)	Fragment3 (Red)	IC_{50} (μ M)	Cluster
985		0.178557	1oit_fragment2	1h01_fragment7	1h01_fragment4	<0.003	1
561		0.355385	2bkz_fragment2	1vyz_fragment3		0.15	2
1047		0.56003	1oiq_fragment3	2c5n_fragment7	1h07_fragment1	0.036	1
67		0.607436	1oiq_fragment3	2c5n_fragment7		4	3
2030		0.615974	2bkz_fragment1	2bkz_fragment2	1vyz_fragment3	0.46	2
1250		1.242246	1oiq_fragment3	2c5n_fragment1	1oiq_fragment1	2.9	3

**Figure 6.** Compound 1250, an initial known inhibitor of CDK2, constructed from fragments of three different known inhibitors.

compound. This rmsd-based scoring function facilitated compound selection from the new compound library.

3.2. CDK2. CDKs are a family of serine/threonine kinases that play significant roles as regulators of cell progression through the consecutive phases of the cell cycle. CDKs are regulated by phosphorylation and activated through their association with

**Figure 7.** Conformation comparison of 1oiq_fragment2 with 2c5n_fragment1 in the active site of CDK2.

cyclins. The precise regulation of CDK activity is essential for the stepwise execution of the many processes required for cell growth and division, including DNA replication and chromosome separation. Abnormal CDK control of the cell cycle has been strongly linked to the molecular pathology of cancer. As such, the CDK family has emerged as an important therapeutic target in the treatment of cancer. CDK2 is a key regulator of the cell cycle, and inhibitors of CDK2 are believed to have potential application as anticancer therapeutics. CDKs share some common structural characteristics, including a low molecular weight (<600), planar aspects, and hydrophobic heterocycle groups.³⁰

Small-molecule CDK2 inhibitors bind in the ATP-binding pocket to exert their inhibitory activity (Figure 2). As is well-documented in the literature, the ATP-binding site comprises the adenine-, ribose-, and phosphate-binding pockets. The adenine-binding pocket is rimmed with the gatekeeper, Phe80, and the hinge region, Glu81—Leu83, and is highly hydrophobic, providing a major scaffold for ATP or inhibitor binding. In Figure 2, the flat plane of the benzodipyrazole occupies this hydrophobic pocket. Glu81 and Leu83 are the hydrogen-bond providers for ATP or inhibitor binding. Nitrogens 6 and 7 in the pyrazole ring A offer and donate a hydrogen bond, respectively, in direct contact with the hinge region. Simultaneously, the carboxamido nitrogen extends into the phosphate pocket, and the sulfamido groups make contacts with the entrance to promote ligand binding.³¹ The interactions with the hinge region and adenine pocket are critical for the inhibitory activity. Thus, the phosphate pocket can be used to improve physicochemical properties and selectivity in lead

optimization. The ligand entrance region can also be used to improve selectivity because of its diverse sequence and conformation.³² The interactions between the ligand and hinge region are significant for determining the inhibitory activity of the ligands, which are also prevalent in other crystal complex structures. Therefore, one hydrogen-bond acceptor and donor and one aromatic ring in the adenine pocket were considered as the key pharmacophoric features (Figure 2) and were all included in the structure-based pharmacophore model developed with Accelrys Discovery Studio 2.5 for filtration.

3.2.1. Fragment Library. At the time this article was prepared, approximately 199 CDK2-inhibitor cocrystal complex structures were available in the Protein Data Bank. Thirty-seven representative complex structures were selected according to the structural diversity of the cocrystallized ligands (Chart 1, inhibitors 1–37)^{31,33–51} and were then superimposed onto the reference structure. Thus, the ligands with their active conformations were also well superimposed within the same coordinate system. The bonds between the carbons and heteroatoms in the ring were set to be cleaved, and the resultant fragment library contained 305 fragments based on the 37 known ligands under the setting rules. The information about their chemical structures was included in the fragment library, as well as about the spatial distribution in the active site. We compared the binding conformation of inhibitor 9 (PDB ID 1OIQ) with its fragments (Figure 3) and found that the ligand was deconstructed into three fragments, all of which maintained the same spatial positions and orientations of the initial ligand.

3.2.2. Evaluation of Fragment-Based Compound Library. New compounds were not allowed to be constructed by all fragments from the same initial compounds. As such, 11958 molecules were generated from 305 fragments. Filtration protocols were applied to remove the redundant compounds and generate a library of good standards, including duplication and drug-likeness filtering. Finally, 814 compounds were selected from the library. Figure 4 demonstrates that the chemical space of the 37 compounds was almost enclosed by the new library compounds with the exception of two ligands, staurosporine and UCN-01, which were extracted from 1AQ1 and 1PKD, respectively. UCN-01, also termed, 7-hydroxystaurosporine, is a staurosporine derivative. Their scaffolds are the same, a big hydrophobic heterocycle plane that covers most space of the ATP-binding pocket, which might result in difficulties for other fragments to link due to the constraints like dihedral angle threshold and others. Overall, the chemical space was much

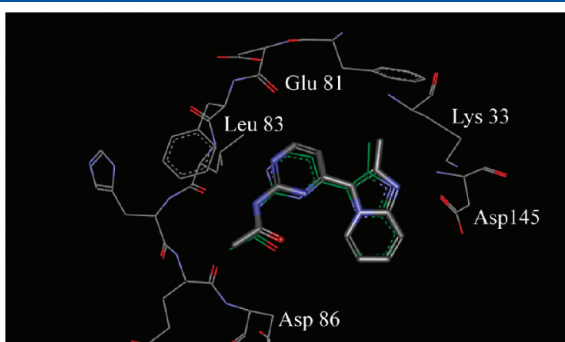


Figure 8. Alignment of the combining (green line) and binding conformations (metal sticks, PDB ID 1OIQ) of compound 1250.

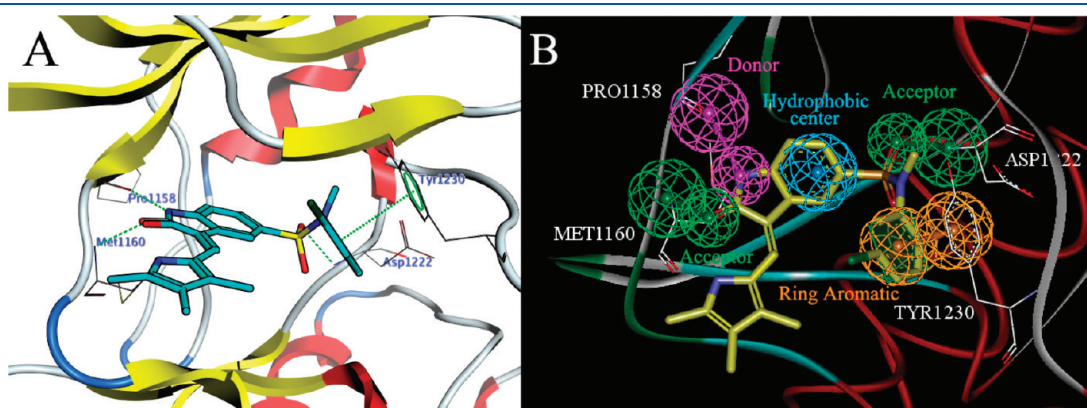
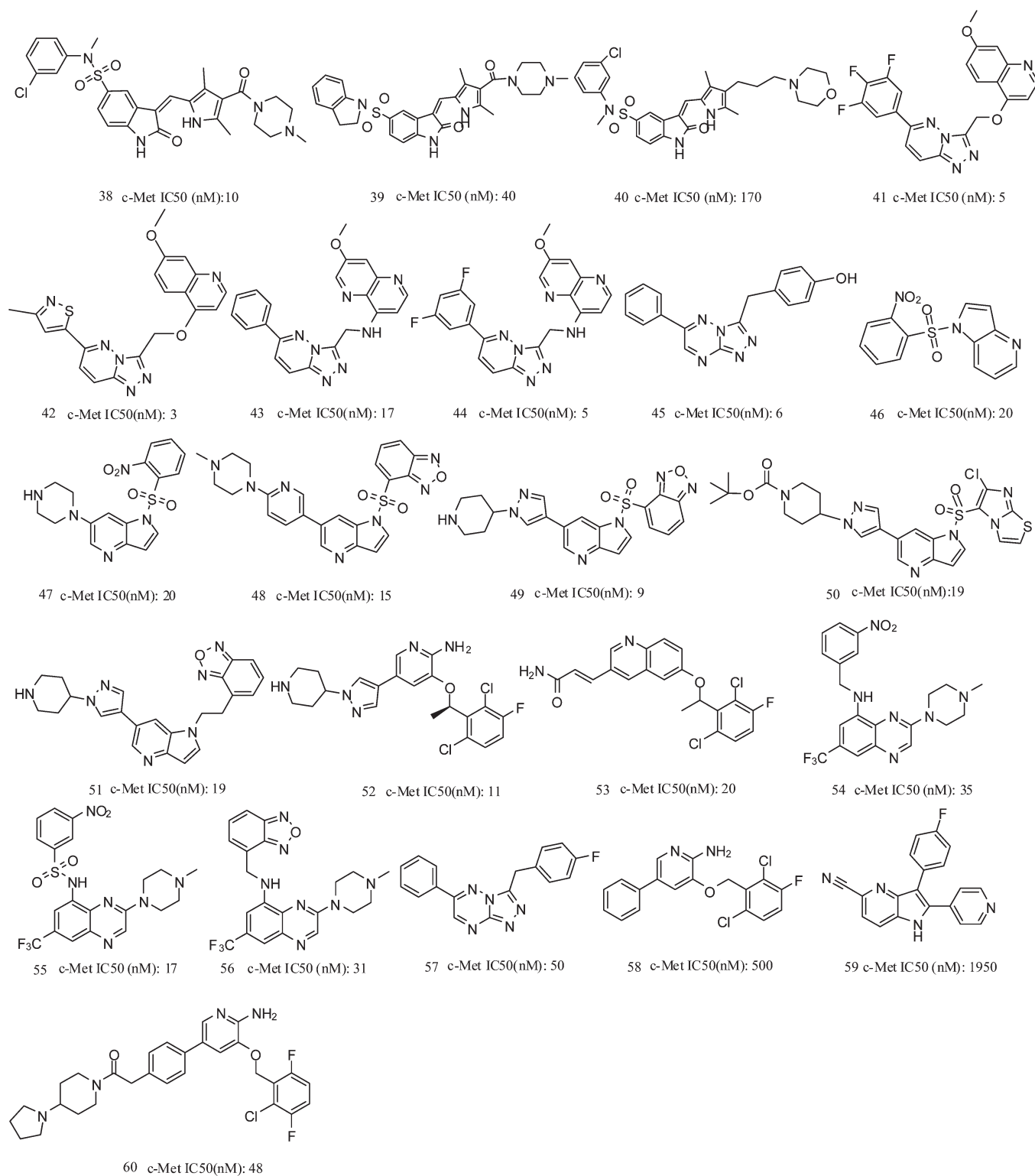


Figure 9. (A) Interactions between the ligand and active site in the crystal complex structure of c-Met (PDB ID 2RFS). (B) Key pharmacophoric constraints in the active site of c-Met.

Chart 2. Two-Dimensional Chemical Structures of 23 Initial c-Met Inhibitors



larger than that enclosed by the initial set, indicating a promising chemical diversity.

The structure-based pharmacophore model was then used to filter the library to find those compounds that match the key pharmacophoric features. One hydrogen donor and acceptor and one aromatic ring, were set as the query that must be

satisfied by new molecules in the library. The compounds were well matched using this model (420 in total) and were subsequently used to perform molecular docking with Glide to select more potentially active inhibitors and predict their binding conformations in the active site. The cocrystal complex structure (PDB ID 1E1X), with a 1.85 resolution was selected to pursue

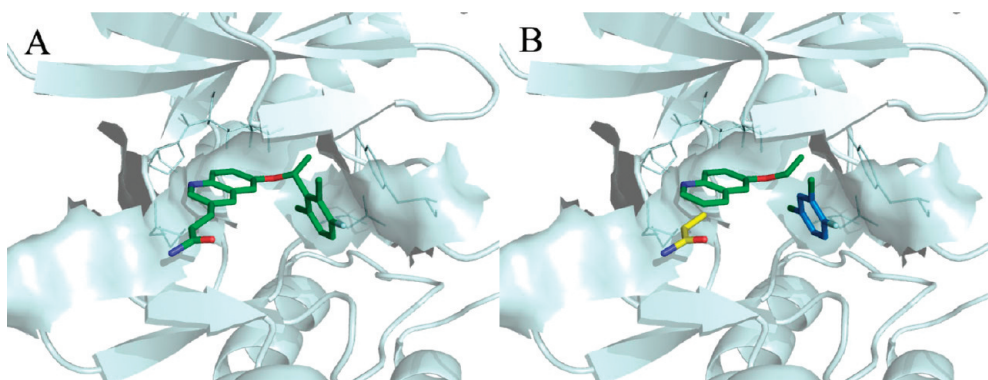


Figure 10. (A) Docking conformation of inhibitor 53. (B) Conformations of the three component fragments deconstructed from inhibitor 53: fragment 1 (yellow), fragment 2 (light green), and fragment 3 (blue).

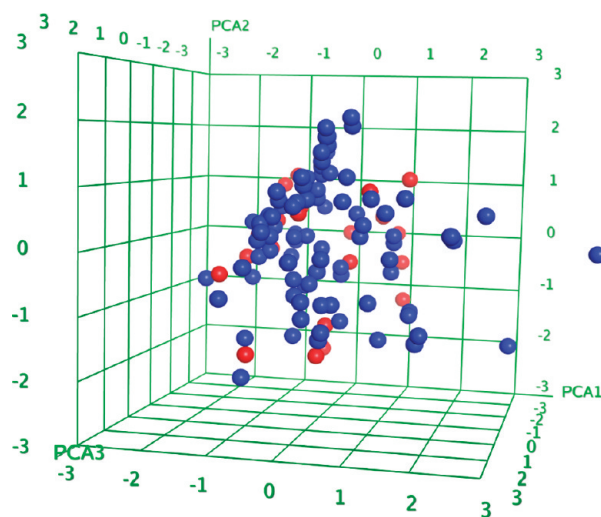


Figure 11. Chemical space covered by the initial 23 known inhibitors (red balls) and the fragment-based compound library (blue balls).

our molecular docking procedure. Additionally, the docking scores (Glide Score) were calculated using the algorithm, and the interactions between the compounds and binding pocket were estimated. Finally, 51 compounds were selected according to Glide Score values and active site binding interactions.

The compound selection criterion determined the quality of the final results. The combining conformations were then generated, and the predicted binding conformations with molecular docking were regarded as their active conformations. The rmsd values between the two conformations were then calculated. From the rmsd value distribution of the 51 compounds, we found that most were located around 2.00, with eight compounds being <1.00 and six >3.00 (Figure 5). Thus, we focused on the compounds that exhibited rmsd values of <3.00. Table 1 lists all the rmsd values of the 51 potential CDK2 inhibitors in ascending order.

Noteworthy, 45 compounds exhibited rmsd values of <3. The following six compounds were synthesized as known CDK2 inhibitors and demonstrated good inhibitory activity (Table 2): compounds- 985,³⁸ -67,³⁸ -1250,³⁸ -1047,³⁸ -2030,³¹ and -561.³¹ According to previous reports, the IC₅₀ values of these inhibitors against CDK2 were all located in the activity range of lead-like compounds.

Compound 1250 possessed the identical chemical structure with that of inhibitor 9, which was presented in the initial known inhibitors set and has been cocrystallized with the protein (PDB ID 1OIQ) with a reported enzymatic IC₅₀ value of 2.9 μm. Furthermore, this inhibitor was not constructed by all the fragments from the initial ligand but by fragments from different initial sets (Figure 6). The fragments that bound in the same region, had similar structures but different spatial positions and orientations, and could serve as alternatives in the fragment combination process. As such, 2c5n_fragment1 took the place of 1oiq_fragment2 in compound 1250, and the distance between the centroids was 0.754 Å (Figure 7). This same strategy was extended for the other newly generated molecules, suggesting that two or more fragments in a close spatial position could form effective molecules by combining with others based on the defined rules. Compound 1250 was almost on the same spatial position with the ligand conformation extracted from 1OIQ (Figure 8) with a rmsd value of 0.3503. From the figure, we observed that the scaffolds were absolutely aligned, and the amide nitrogen provided an H-bond to Leu83 in the complex structure almost in the initial place. This could be a representative case in the fragment-based compound library, which showed a good reproducibility of the ligand conformations within the cocrystal complexes. The rmsd value between the combining and docking conformation was 1.242246, which was ranked tenth in Table 1. This value was a little higher than that between the combining and cocrystal conformations, illustrating that the fragments in the initial place still played important roles in protein–ligand binding for the construction of new compounds. The structural and conformational similarity comparison showed that our method could reproduce not only the same chemical structure of this inhibitor in the initial set, but also the pharmacophoric conformation.

The five compounds ranked at the first six places in Table 1, which did not possess cocrystal structures with CDK2, were also constructed with the fragments from the different initial inhibitors (Table 2) and have been reported as CDK2 inhibitors with good activities. Deviations between their combining and binding conformations predicted with molecular docking were small and in the range of 0.178557 to 0.615974, indicating that all fragments maintained their initial conformation and orientation in the newly constructed compounds and contributed additively to the protein–ligand binding interaction.

These small rmsd values confirmed that our strategy could reproduce both cocrystallized inhibitors in the initial set and other external active inhibitors. Comparison between their

Table 3. Ranking of the 47 Potentially Active Compounds Using the rmsd Values

ranking	index	name	rmsd	cluster	ranking	index	name	rmsd	cluster
1	18	compound 78	0.33842	5	25 ^a	6	compound 433	1.730309	2
2 ^b	4	compound 377	0.520095	5	26	46	compound 56	1.842219	1
3	13	compound 385	0.591342	5	27	47	compound 65	2.000136	1
4	45	compound 108	1.225447	5	28	44	compound 481	2.057362	4
5	28	compound 34	1.257521	1	29	7	compound 488b	2.091561	2
6 ^a	1	compound 50	1.291261	1	30	27	compound 223	2.126921	5
7	43	compound 397	1.303848	5	31	29	compound 511	2.149703	4
8	36	compound 293	1.311509	1	32	8	compound 392	2.149963	2
9	17	compound 239	1.40912	1	33	25	compound 1052	2.195663	4
10	37	compound 285	1.428585	1	34	30	compound 136	2.218499	4
11 ^b	3	compound 251	1.460918	1	35	34	compound 861	2.29331	5
12	26	compound 477	1.469694	4	36	32	compound 544	2.297742	5
13	24	compound 334	1.485797	1	37	20	compound 117	2.31773	4
14	38	compound 162	1.527111	1	38	11	compound 1051	2.349423	2
15	10	compound 1042	1.559403	5	39	21	compound 104	2.411815	3
16	16	compound 235	1.587853	1	40	5	compound 391 ^b	2.517173	2
17	39	compound 95	1.588193	4	41	9	compound 476	2.527462	2
18	35	compound 208	1.60972	1	42	33	compound 1054	2.605567	4
19	14	compound 83	1.661658	2	43 ^a	2	compound 123	2.613489	2
20	19	compound 105	1.669986	3	44	40	compound 516	2.677985	4
21	23	compound 103	1.687282	3	45	31	compound 80	2.796974	4
22	15	compound 88	1.694477	2	46	41	compound 473	3.097218	4
23	12	compound 257	1.697311	1	47	42	compound 988	3.783284	5
24	22	compound 478	1.718174	4					

^a Compounds belonging to external known inhibitors, not including in the initial c-Met inhibitor set. ^b Compounds belonging to the initial c-Met inhibitor set.

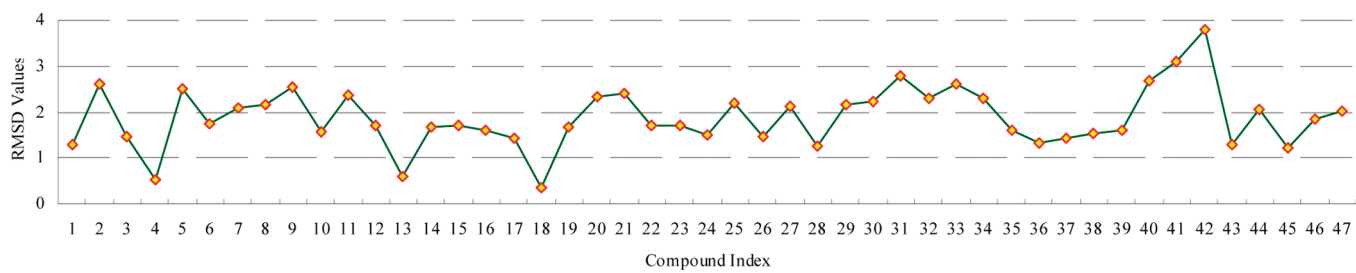


Figure 12. rmsd value distribution of the 47 potential compounds against c-Met.

conformation types also showed small deviations, which is consistent with the cocrystallized compound 1250, demonstrating good reproducibility of their binding conformations and orientations. Finally, the compounds in Table 1 were categorized into three groups using molecule cluster module analyses to identify the compounds with common structural characters. Novel potential compounds were also contained in the new molecular library, which showed preferred spatial orientation, the lowest structural similarity, and rmsd values. The six known inhibitors located in each cluster were considered as representative compounds and were used as the references for selecting potential leads, which demonstrated high pharmacophoric similarity and were ranked around the representative known compounds.

3.3. c-MET. The receptor tyrosine kinase, c-Met (i.e., mesenchymal–epithelial transition factor), and its natural ligand, hepatocyte growth factor (HGF), are involved in cell proliferation, migration, and invasion, which are essential for normal embryonic

development. However, c-Met has been shown to be deregulated and associated with high tumor grade and poor prognosis in a number of human cancers. Several mechanisms lead to deregulation, including the overexpression of c-Met and/or HGF, amplification of the Met gene, or activating mutations of c-Met, all of which have been found in human cancers. Currently, there are several ATP-competitive, c-Met kinase inhibitor types, developed based on different scaffolds, including 7-azaindoles, aminopyridines, and triazolopyridazines.⁵² The gatekeeper of this active site is Leu1157, which is comparatively smaller than Phe80 in CDK2. The binding modes of the inhibitors were divided into two different type-based interactions deep within the hydrophobic active site in front of Leu1157. The compounds of the first type, which did not bind in this pocket, were selected as the materials for fragment generation. From Figure 9, we found the following common binding modes of them: (1) hydrogen bonding, hinge region (Pro1158 and Met1160); (2) hydrophobic and $\pi-\pi$

Table 4. Seven Known c-Met Inhibitors Generated by This Strategy

Comp. No.	Structures	RMSD	Frgment1 (Red)	Frgment2 (Blue)	Frgment3 (Green)	IC ₅₀ (nm)	Cluster
377		0.520095	58_fragment1	57_fragment1	57_fragment5	50	5
251		1.460918	43_fragment1	42_fragment2	42_fragment3	6	1
488		2.091561	53_fragment3	53_fragment1	52_fragment2	20	2
391		2.517173	58_fragment3	60_fragment1	53_fragment2	500	2
50		1.291261		57_fragment1	42_fragment3	56	1
433		1.730309	58_fragment3	60_fragment1	60_fragment6	640	2
123		2.613489		53_fragment1	52_fragment2	1200	2

interactions, Tyr1230; and (3) hydrogen bonding, Asp1222. The first type of c-Met inhibitors usually covers these regions of the ATP-binding pocket.⁵³ These important protein–ligand interactions were also included in the structure-based pharmacophore to be used in compound library filtration.

3.3.1. Fragment Library. C-Met is an important target, and several crystallized complex structures have been reported. Twenty-three representative c-Met inhibitors (Chart 2, inhibitors 38–60)^{54–59} with type-1 binding modes were selected to construct the initial set. After being docked into the same binding pocket, the docking conformations were well-aligned and were then deconstructed into fragments. The other parameter settings were identical to those used for the CDK2 studies; the bonds between the carbon and heteroatoms in a ring were not allowed to be broken. With these settings, 118 fragments were obtained from the 23 known c-Met inhibitors. Inhibitor 53, shown in

Figure 10, was deconstructed into three fragments. The scaffold, which made contact with the hinge region, remained in the adenine-binding pocket. Fragment 1, propionamide, was near the solvent-accessible region. The halogenated phenyl was also near Tyr1230. All fragments generated from inhibitor 53 remained in the active site. The other selected known inhibitors were also deconstructed into small fragments in the same way. The spatial and structural information contained in these fragments were sufficiently used in the fragment combining procedure.

3.3.2. Evaluation of Fragment-Based Compound Library. The combining process afforded 1104 compounds, which were obtained from the 118 fragments. After the duplication and drug-likeness filtration, only 92 of them were retained to construct a compound library. Similarly, the selected two-dimensional descriptors that described the atomic nature, molecular size, polarity, lipophilicity, and flexibility were first calculated. The

chemical space coverage was also presented after graphical distributions of the data sets had been constructed in the three-dimensional space. Figure 11 demonstrates that the chemical space covered by the 23 known c-Met inhibitors was all located in the region covered by the fragment-based compound library. Four compounds fell outside the PCA axes because they exhibited lower molecular weights than the known c-Met inhibitors. This analysis once again confirmed that the chemical space could be maximally probed with FBDD. Additionally, the compounds in the newly constructed library had physical and chemical properties similar to those of the initial known inhibitors, indicating that potential novel inhibitors might exist among them.

Unlike for the observed CDK2 data, all pharmacophoric features presented in Figure 9B were prevalent in the other crystal structures. Therefore, all of these features were retained in the structure-based pharmacophore model used as the query in molecular library filtration. Eighty-two compounds satisfied at least four of the five specified pharmacophoric features. The cocrystal complex structure (PDB ID 3ISN)⁵⁶ with a 2.00 resolution was selected to pursue our molecular docking procedure. The active-site docking conformations of the new molecules, which could be considered as their binding conformations, were then determined. Forty-seven of these compounds were selected according to their binding modes and Glide scores. The rmsd values between their combining and docking conformations were then calculated to evaluate the deviations. A low deviation between these two conformation types indicated a high probability of being a potential active inhibitor. Table 3 lists the rmsd values of the 47 potential c-Met inhibitors in ascending order. From the rmsd value distribution shown in Figure 12, we determined that most of the potential c-Met inhibitors were located at approximately 2.00, three at <1.00, and two at >3.00. Thus, we focused on compounds with rmsd values of <3.00.

Forty-five new compounds exhibited rmsd values of <3.00, seven of which are known c-Met inhibitors with good inhibitory activities (Table 4). Four of the 23 initial known inhibitors (i.e., inhibitors 57,⁵² 45,⁵⁸ 53,⁵⁴ and 58⁵²) were reproduced. These compounds had the same chemical structures as compounds 377, 251, 488, and 391, respectively, in the newly constructed compound library. The other three known c-Met inhibitors, not in the initial set, were also reproduced, and their inhibitory activities were 56,⁵² 640,⁵² and 1200 nm.⁵⁴ All of these inhibitors were not cocrystallized with the protein. We used only their docking conformations to analyze the deviation of their binding modes. The rmsd values between the docking and combining conformations (Table 4) indicated acceptable deviations. Additionally, the inhibitors with good inhibitory activity were almost highly ranked. The acceptable rmsd values suggested that the new compound fragments almost maintained their initial spatial positions and orientations in the active site. The differently colored fragments from the initial inhibitors, which were used to construct these seven reproduced known inhibitors, are listed in Table 4.

This high reproducibility confirmed that the active inhibitors could also be produced using the docking conformations as the starting points. The novel compounds that exhibited less chemical structural similarity but high pharmacophoric and shape similarity to the known inhibitors are also included in Table 3. All compounds, including the seven known inhibitors, were categorized into five clusters according to their common structural characters. Other new compounds with similar rmsd values around the known ones might exhibit comparable or even better inhibitory activity.

4. CONCLUSIONS

We have implemented a fragment-based strategy for lead generation and presented good solutions to the current problems in FBBD. Rules similar to those used in RECAP were applied in fragment generation with a few obvious differences. The binding conformations of the fragments from the initial inhibitors were retained after the aligned known inhibitors from the cocrystal or docking complex structures had been deconstructed. Suitable three-dimensional fragments that bound simultaneously to separate regions of the binding site were obtained to satisfy the primary requirement of this strategy. Novel molecules were constructed after neighboring spatial fragments were linked or merged, and the requirement of selecting substituted points or groups was unnecessary, reducing artificial disturbance. The binding conformations of the novel molecules might have been different from the combined conformations determined by their component fragments. Thus, the rmsd values were calculated to evaluate the individual binding mode distortions of the component fragments in the final compounds. The rmsd-based scoring function was used as the main criterion for lead selection.

Our strategy was validated by applying this fragment-based method to test the novel CDK2 and c-Met inhibitors. The workflow was independently applied to the two initial inhibitor sets to generate novel molecular libraries with high quality. The known inhibitors within and outside of the initial sets and the binding mode of the cocrystal ligand were successfully reproduced. The reproduced known inhibitors, which showed good activities, were then used in lead selection. Based on the rmsd-based scoring function, the lower the rmsd value, the more promising a novel molecule is. The low rmsd values of the novel constructed compounds demonstrated that fragments were combined with only small distortions using our strategy. Although the cocrystal complex structures were the best choices to obtain binding conformations, accurate molecular docking could be a qualified alternative. Thus, the two cases of CDK2 and c-Met inhibitors are good examples of the effective use of this strategy in drug discovery. The binding modes of these known inhibitors that were derived from crystal structures and predicted with accurate molecular docking achieved similar effects, showing that this strategy could be efficiently applied to targets with numbers of or only several cocrystal complex structures. New inhibitors with novel structures were added to the initial library set and will greatly increase the novelty of this fragment and fragment-based compound library. This efficient and effective strategy could be an invaluable tool in the discovery and optimization of potential drug leads against specific targets.

■ AUTHOR INFORMATION

Corresponding Author

*Phone: 86-25-86185163. Fax: 86-25-86185179. E-mail: ydchen@cpu.edu.cn.

■ ACKNOWLEDGMENT

The authors thank Dr. Hufang Li and Dr. Shulin Zhuang for their help in drafting the manuscript. This work was financially supported by the National Natural Science Foundation of China (30973609); the Natural Science Foundation of Jiangsu Province, China (BK2009303); the National Major Science and Technology Project of China (Innovation and Development of

New Drugs, No. 2009ZX09501-003); and the Qing Lan Project of Jiangsu Province, China.

■ REFERENCES

- (1) Rees, D. C.; Congreve, M.; Murray, C. W.; Carr, R. Fragment-based lead discovery. *Nat. Rev. Drug Discov.* **2004**, *3*, 660–672.
- (2) Erlanson, D. A.; Hansen, S. K. Making drugs on proteins: Site-directed ligand discovery for fragment-based lead assembly. *Curr. Opin. Chem. Biol.* **2004**, *8*, 399–406.
- (3) Verdonk, M. L.; Hartshorn, M. J. Structure-guided fragment screening for lead discovery. *Curr. Opin. Drug Discov. Dev.* **2004**, *7*, 404–410.
- (4) Zartler, E. R.; Shapiro, M. J. Fragonomics: Fragment-based drug discovery. *Curr. Opin. Chem. Biol.* **2005**, *9*, 366–370.
- (5) Boehm, H. J.; Boehringer, M.; Bur, D.; Gmuender, H.; Huber, W.; Klaus, W.; Kostrewa, D.; Kuehne, H.; Luebbers, T.; Meunier-Keller, N.; Mueller, F. Novel inhibitors of DNA gyrase: 3D structure based biased needle screening, hit validation by biophysical methods, and 3D guided optimization. A promising alternative to random screening. *J. Med. Chem.* **2000**, *43*, 2664–2674.
- (6) Shelke, S. V.; Cutting, B.; Jiang, X.; Koliwer-Brandl, H.; Strasser, D. S.; Schwardt, O.; Kelm, S.; Ernst, B. A fragment-based in situ combinatorial approach to identify high-affinity ligands for unknown binding sites. *Angew. Chem., Int. Ed.* **2010**, *49*, S721–S725.
- (7) Verlinde, C. L.; Rudenko, G.; Hol, W. G. In search of new lead compounds for trypanosomiasis drug design: A protein structure-based linked-fragment approach. *J. Comput.-Aided Mol. Des.* **1992**, *6*, 131–147.
- (8) Shuker, S. B.; Hajduk, P. J.; Meadows, R. P.; Fesik, S. W. Discovering high-affinity ligands for proteins: SAR by NMR. *Science* **1996**, *274*, 1531–1534.
- (9) Oltersdorf, T.; Elmore, S. W.; Shoemaker, A. R.; Armstrong, R. C.; Augeri, D. J.; Belli, B. A.; Bruncko, M.; Deckwerth, T. L.; Dinges, J.; Hajduk, P. J.; Joseph, M. K.; Kitada, S.; Korsmeyer, S. J.; Kunzer, A. R.; Letai, A.; Li, C.; Mitten, M. J.; Nettelesheim, D. G.; Ng, S.; Nimmer, P. M.; O'Connor, J. M.; Oleksijew, A.; Petros, A. M.; Reed, J. C.; Shen, W.; Tahir, S. K.; Thompson, C. B.; Tomaselli, K. J.; Wang, B.; Wendt, M. D.; Zhang, H.; Fesik, S. W.; Rosenberg, S. H. An inhibitor of Bcl-2 family proteins induces regression of solid tumours. *Nature* **2005**, *435*, 677–681.
- (10) Hajduk, P. J.; Greer, J. A decade of fragment-based drug design: Strategic advances and lessons learned. *Nat. Rev. Drug Discov.* **2007**, *6*, 211–219.
- (11) Kolb, P.; Caflisch, A. Automatic and efficient decomposition of two-dimensional structures of small molecules for fragment-based high-throughput docking. *J. Med. Chem.* **2006**, *49*, 7384–7392.
- (12) Warren, G. L.; Andrews, C. W.; Capelli, A. M.; Clarke, B.; LaLonde, J.; Lambert, M. H.; Lindvall, M.; Nevins, N.; Semus, S. F.; Senger, S.; Tedesco, G.; Wall, I. D.; Woolven, J. M.; Peishoff, C. E.; Head, M. S. A critical assessment of docking programs and scoring functions. *J. Med. Chem.* **2006**, *49*, 5912–5931.
- (13) Lewell, X. Q.; Judd, D. B.; Watson, S. P.; Hann, M. M. RECAP—Retrosynthetic combinatorial analysis procedure: A powerful new technique for identifying privileged molecular fragments with useful applications in combinatorial chemistry. *J. Chem. Inf. Comput. Sci.* **1998**, *38*, 511–522.
- (14) Congreve, M.; Chessari, G.; Tisi, D.; Woodhead, A. J. Recent developments in fragment-based drug discovery. *J. Med. Chem.* **2008**, *51*, 3661–3680.
- (15) Knox, A. J.; Price, T.; Pawlak, M.; Golfis, G.; Flood, C. T.; Fayne, D.; Williams, D. C.; Meegan, M. J.; Lloyd, D. G. Integration of ligand and structure-based virtual screening for the identification of the first dual targeting agent for heat shock protein 90 (Hsp90) and tubulin. *J. Med. Chem.* **2009**, *52*, 2177–2180.
- (16) Lloyd, D. G.; Golfis, G.; Knox, A. J.; Fayne, D.; Meegan, M. J.; Oprea, T. I. Oncology exploration: Charting cancer medicinal chemistry space. *Drug Discov. Today* **2006**, *11*, 149–159.
- (17) Chemical Computing Group. <http://www.chemcomp.com> (accessed Mar 17, 2010).
- (18) Lipinski, C. A. Lead- and drug-like compounds: The rule-of-five revolution. *Drug Discov. Today: Technol.* **2004**, *1*, 337–341.
- (19) Kontoyianni, M.; McClellan, L. M.; Sokol, G. S. Evaluation of docking performance: Comparative data on docking algorithms. *J. Med. Chem.* **2004**, *47*, 558–565.
- (20) Sandor, M.; Kiss, R.; Keseru, G. M. Virtual fragment docking by Glide: A validation study on 190 protein-fragment complexes. *J. Chem. Inf. Model.* **2010**, *50*, 1165–1172.
- (21) Law, R.; Barker, O.; Barker, J. J.; Hesterkamp, T.; Godemann, R.; Andersen, O.; Fryatt, T.; Courtney, S.; Hallett, D.; Whittaker, M. The multiple roles of computational chemistry in fragment-based drug design. *J. Comput.-Aided Mol. Des.* **2009**, *23*, 459–473.
- (22) Babaoglu, K.; Shoichet, B. K. Deconstructing fragment-based inhibitor discovery. *Nat. Chem. Biol.* **2006**, *2*, 720–723.
- (23) Hajduk, P. J. Puzzling through fragment-based drug design. *Nat. Chem. Biol.* **2006**, *2*, 658–659.
- (24) Barelier, S.; Pons, J.; Marcillat, O.; Lancelin, J. M.; Krimm, I. Fragment-based deconstruction of Bcl-xL inhibitors. *J. Med. Chem.* **2010**, *53*, 2577–2588.
- (25) Jahnke, W.; Florsheimer, A.; Blommers, M. J.; Paris, C. G.; Heim, J.; Nalin, C. M.; Perez, L. B. Second-site NMR screening and linker design. *Curr. Top. Med. Chem.* **2003**, *3*, 69–80.
- (26) Chen, J.; Zhang, Z.; Stebbins, J. L.; Zhang, X.; Hoffman, R.; Moore, A.; Pellecchia, M. A fragment-based approach for the discovery of isoform-specific p38 α inhibitors. *ACS. Chem. Biol.* **2007**, *2*, 329–336.
- (27) Hajduk, P. J.; Greer, J. A decade of fragment-based drug design: Strategic advances and lessons learned. *Nat. Rev. Drug Discov.* **2007**, *6*, 211–219.
- (28) Saxty, G.; Woodhead, S. J.; Berdini, V.; Davies, T. G.; Verdonk, M. L.; Wyatt, P. G.; Boyle, R. G.; Barford, D.; Downham, R.; Garrett, M. D.; Carr, R. A. Identification of inhibitors of protein kinase B using fragment-based lead discovery. *J. Med. Chem.* **2007**, *50*, 2293–2296.
- (29) Ciulli, A.; Abell, C. Fragment-based approaches to enzyme inhibition. *Curr. Opin. Biotechnol.* **2007**, *18*, 489–496.
- (30) Vulpetti, A.; Pevarello, P. An analysis of the binding modes of ATP-competitive CDK2 inhibitors as revealed by X-ray structures of protein-inhibitor complexes. *Curr. Med. Chem. Anticancer Agents* **2005**, *5*, 561–573.
- (31) D'Alessio, R.; Bargiotti, A.; Metz, S.; Brasca, M. G.; Cameron, A.; Ermoli, A.; Marsiglio, A.; Polucci, P.; Roletto, F.; Tibolla, M.; Vazquez, M. L.; Vulpetti, A.; Pevarello, P. Benzodipyrazoles: A new class of potent CDK2 inhibitors. *Bioorg. Med. Chem. Lett.* **2005**, *15*, 1315–1319.
- (32) Liao, J. J. Molecular recognition of protein kinase binding pockets for design of potent and selective kinase inhibitors. *J. Med. Chem.* **2007**, *50*, 409–424.
- (33) Lawrie, A. M.; Noble, M. E.; Tunnah, P.; Brown, N. R.; Johnson, L. N.; Endicott, J. A. Protein kinase inhibition by staurosporine revealed in details of the molecular interaction with CDK2. *Nat. Struct. Biol.* **1997**, *4*, 796–801.
- (34) Kontopidis, G.; McInnes, C.; Pandalaneni, S. R.; McNae, I.; Gibson, D.; Mezna, M.; Thomas, M.; Wood, G.; Wang, S.; Walkinshaw, M. D.; Fischer, P. M. Differential binding of inhibitors to active and inactive CDK2 provides insights for drug design. *Chem. Biol.* **2006**, *13*, 201–211.
- (35) Richardson, C. M.; Williamson, D. S.; Parratt, M. J.; Borgognoni, J.; Cansfield, A. D.; Dokurno, P.; Francis, G. L.; Howes, R.; Moore, J. D.; Murray, J. B.; Robertson, A.; Surgenor, A. E.; Torrance, C. J. Triazolo[1,5-a]pyrimidines as novel CDK2 inhibitors: Protein structure-guided design and SAR. *Bioorg. Med. Chem. Lett.* **2006**, *16*, 1353–1357.
- (36) Beattie, J. F.; Breault, G. A.; Ellston, R. P.; Green, S.; Jewsbury, P. J.; Midgley, C. J.; Naven, R. T.; Minshull, C. A.; Paupit, R. A.; Tucker, J. A.; Pease, J. E. Cyclin-dependent kinase 4 inhibitors as a treatment for cancer. Part 1: Identification and optimization of substituted 4,6-bis anilino pyrimidines. *Bioorg. Med. Chem. Lett.* **2003**, *13*, 2955–2960.
- (37) Breault, G. A.; Ellston, R. P.; Green, S.; James, S. R.; Jewsbury, P. J.; Midgley, C. J.; Paupit, R. A.; Minshull, C. A.; Tucker, J. A.; Pease,

- J. E. Cyclin-dependent kinase 4 inhibitors as a treatment for cancer. Part 2: Identification and optimization of substituted 2,4-bis anilino pyrimidines. *Bioorg. Med. Chem. Lett.* **2003**, *13*, 2961–2966.
- (38) Anderson, M.; Beattie, J. F.; Breault, G. A.; Breed, J.; Byth, K. F.; Culshaw, J. D.; Ellston, R. P.; Green, S.; Minshull, C. A.; Norman, R. A.; Paupert, R. A.; Stanway, J.; Thomas, A. P.; Jewsbury, P. J. Imidazo[1,2-a]pyridines: A potent and selective class of cyclin-dependent kinase inhibitors identified through structure-based hybridisation. *Bioorg. Med. Chem. Lett.* **2003**, *13*, 3021–3026.
- (39) Liu, J. J.; Dermatakis, A.; Lukacs, C.; Konzelmann, F.; Chen, Y.; Kammlott, U.; Depinto, W.; Yang, H.; Yin, X.; Schutt, A.; Simcox, M. E.; Luk, K. C. 3,5,6-Trisubstituted naphthostyryls as CDK2 inhibitors. *Bioorg. Med. Chem. Lett.* **2003**, *13*, 2465–2468.
- (40) Johnson, L. N.; De Moliner, E.; Brown, N. R.; Song, H.; Barford, D.; Endicott, J. A.; Noble, M. E. Structural studies with inhibitors of the cell cycle regulatory kinase cyclin-dependent protein kinase 2. *Pharmacol. Ther.* **2002**, *93*, 113–124.
- (41) Moshinsky, D. J.; Bellamacina, C. R.; Boisvert, D. C.; Huang, P.; Hui, T.; Jancarik, J.; Kim, S. H.; Rice, A. G. SU9516: Biochemical analysis of cdk inhibition and crystal structure in complex with cdk2. *Biochem. Biophys. Res. Commun.* **2003**, *310*, 1026–1031.
- (42) Wang, S.; Meades, C.; Wood, G.; Osnowski, A.; Anderson, S.; Yuill, R.; Thomas, M.; Mezna, M.; Jackson, W.; Midgley, C.; Griffiths, G.; Fleming, I.; Green, S.; McNae, I.; Wu, S. Y.; McInnes, C.; Zheleva, D.; Walkinshaw, M. D.; Fischer, P. M. 2-Anilino-4-(thiazol-5-yl)pyrimidine CDK inhibitors: Synthesis, SAR analysis, X-ray crystallography, and biological activity. *J. Med. Chem.* **2004**, *47*, 1662–1675.
- (43) Luk, K. C.; Simcox, M. E.; Schutt, A.; Rowan, K.; Thompson, T.; Chen, Y.; Kammlott, U.; DePinto, W.; Dunten, P.; Dermatakis, A. A new series of potent oxindole inhibitors of CDK2. *Bioorg. Med. Chem. Lett.* **2004**, *14*, 913–917.
- (44) Byth, K. F.; Cooper, N.; Culshaw, J. D.; Heaton, D. W.; Oakes, S. E.; Minshull, C. A.; Norman, R. A.; Paupert, R. A.; Tucker, J. A.; Breed, J.; Pannifer, A.; Rowsell, S.; Stanway, J. J.; Valentine, A. L.; Thomas, A. P. Imidazo[1,2-b]pyridazines: A potent and selective class of cyclin-dependent kinase inhibitors. *Bioorg. Med. Chem. Lett.* **2004**, *14*, 2249–2252.
- (45) Pevarello, P.; Brasca, M. G.; Amici, R.; Orsini, P.; Traquandi, G.; Corti, L.; Piutti, C.; Sansonna, P.; Villa, M.; Pierce, B. S.; Pulici, M.; Giordano, P.; Martina, K.; Fritzen, E. L.; Nugent, R. A.; Casale, E.; Cameron, A.; Ciomei, M.; Roletto, F.; Isacchi, A.; Fogliatto, G.; Pesenti, E.; Pastori, W.; Marsiglio, A.; Leach, K. L.; Clare, P. M.; Fiorentini, F.; Varasi, M.; Vulpetti, A.; Warpehoski, M. A. 3-Aminopyrazole inhibitors of CDK2/cyclin A as antitumor agents. 1. Lead finding. *J. Med. Chem.* **2004**, *47*, 3367–3380.
- (46) Williamson, D. S.; Parratt, M. J.; Bower, J. F.; Moore, J. D.; Richardson, C. M.; Dokurno, P.; Cansfield, A. D.; Francis, G. L.; Hebdon, R. J.; Howes, R.; Jackson, P. S.; Lockie, A. M.; Murray, J. B.; Nunns, C. L.; Powles, J.; Robertson, A.; Surgenor, A. E.; Torrance, C. J. Structure-guided design of pyrazolo[1,5-a]pyrimidines as inhibitors of human cyclin-dependent kinase 2. *Bioorg. Med. Chem. Lett.* **2005**, *15*, 863–867.
- (47) Yue, E. W.; DiMeo, S. V.; Higley, C. A.; Markwalder, J. A.; Burton, C. R.; Benfield, P. A.; Grafstrom, R. H.; Cox, S.; Muckelbauer, J. K.; Smallwood, A. M.; Chen, H.; Chang, C. H.; Trainor, G. L.; Seitz, S. P. Synthesis and evaluation of indenopyrazoles as cyclin-dependent kinase inhibitors. Part 4: Heterocycles at C3. *Bioorg. Med. Chem. Lett.* **2004**, *14*, 343–346.
- (48) Sielecki, T. M.; Johnson, T. L.; Liu, J.; Muckelbauer, J. K.; Grafstrom, R. H.; Cox, S.; Boylan, J.; Burton, C. R.; Chen, H.; Smallwood, A.; Chang, C. H.; Boisclair, M.; Benfield, P. A.; Trainor, G. L.; Seitz, S. P. Quinazolines as cyclin dependent kinase inhibitors. *Bioorg. Med. Chem. Lett.* **2001**, *11*, 1157–1160.
- (49) Yue, E. W.; Higley, C. A.; DiMeo, S. V.; Carini, D. J.; Nugiel, D. A.; Benware, C.; Benfield, P. A.; Burton, C. R.; Cox, S.; Grafstrom, R. H.; Sharp, D. M.; Sisk, L. M.; Boylan, J. F.; Muckelbauer, J. K.; Smallwood, A. M.; Chen, H.; Chang, C. H.; Seitz, S. P.; Trainor, G. L. Synthesis and evaluation of indenopyrazoles as cyclin-dependent kinase inhibitors. 3. Structure activity relationships at C3(1,2). *J. Med. Chem.* **2002**, *45*, 5233–5248.
- (50) Pratt, D. J.; Bentley, J.; Jewsbury, P.; Boyle, F. T.; Endicott, J. A.; Noble, M. E. Dissecting the determinants of cyclin-dependent kinase 2 and cyclin-dependent kinase 4 inhibitor selectivity. *J. Med. Chem.* **2006**, *49*, 5470–5477.
- (51) Richardson, C. M.; Nunns, C. L.; Williamson, D. S.; Parratt, M. J.; Dokurno, P.; Howes, R.; Borgognoni, J.; Drysdale, M. J.; Finch, H.; Hubbard, R. E.; Jackson, P. S.; Kierstan, P.; Lentzen, G.; Moore, J. D.; Murray, J. B.; Simmonite, H.; Surgenor, A. E.; Torrance, C. J. Discovery of a potent CDK2 inhibitor with a novel binding mode, using virtual screening and initial, structure-guided lead scoping. *Bioorg. Med. Chem. Lett.* **2007**, *17*, 3880–3885.
- (52) Underiner, T. L.; Herbertz, T.; Miknyoczki, S. J. Discovery of small molecule c-Met inhibitors: Evolution and profiles of clinical candidates. *Anticancer Agents Med. Chem.* **2010**, *10*, 7–27.
- (53) Bellon, S. F.; Kaplan-Lefko, P.; Yang, Y.; Zhang, Y.; Moriguchi, J.; Rex, K.; Johnson, C. W.; Rose, P. E.; Long, A. M.; O'Connor, A. B.; Gu, Y.; Coxon, A.; Kim, T. S.; Tasker, A.; Burgess, T. L.; Dussault, I. c-Met inhibitors with novel binding mode show activity against several hereditary papillary renal cell carcinoma-related mutations. *J. Biol. Chem.* **2008**, *283*, 2675–2683.
- (54) Nishii, H.; Chiba, T.; Morikami, K.; Fukami, T. A.; Sakamoto, H.; Ko, K.; Koyano, H. Discovery of 6-benzylxyquinolines as c-Met selective kinase inhibitors. *Bioorg. Med. Chem. Lett.* **2010**, *20*, 1405–1409.
- (55) Christensen, J. G.; Burrows, J.; Salgia, R. c-Met as a target for human cancer and characterization of inhibitors for therapeutic intervention. *Cancer Lett.* **2005**, *225*, 1–26.
- (56) Boezio, A. A.; Berry, L.; Albrecht, B. K.; Bauer, D.; Bellon, S. F.; Bode, C.; Chen, A.; Choquette, D.; Dussault, I.; Fang, M.; Hirai, S.; Kaplan-Lefko, P.; Larrow, J. F.; Lin, M. H.; Lohman, J.; Potashman, M. H.; Qu, Y.; Rex, K.; Santostefano, M.; Shah, K.; Shimanovich, R.; Springer, S. K.; Teffera, Y.; Yang, Y.; Zhang, Y.; Harmange, J. C. Discovery and optimization of potent and selective triazolopyridazine series of c-Met inhibitors. *Bioorg. Med. Chem. Lett.* **2009**, *19*, 6307–6312.
- (57) Albrecht, B. K.; Harmange, J. C.; Bauer, D.; Berry, L.; Bode, C.; Boezio, A. A.; Chen, A.; Choquette, D.; Dussault, I.; Fridrich, C.; Hirai, S.; Hoffman, D.; Larrow, J. F.; Kaplan-Lefko, P.; Lin, J.; Lohman, J.; Long, A. M.; Moriguchi, J.; O'Connor, A.; Potashman, M. H.; Reese, M.; Rex, K.; Siegmund, A.; Shah, K.; Shimanovich, R.; Springer, S. K.; Teffera, Y.; Yang, Y.; Zhang, Y.; Bellon, S. F. Discovery and optimization of triazolopyridazines as potent and selective inhibitors of the c-Met kinase. *J. Med. Chem.* **2008**, *51*, 2879–2882.
- (58) Porter, J.; Lumb, S.; Franklin, R. J.; Gascon-Simorte, J. M.; Calmiano, M.; Riche, K. L.; Lallemand, B.; Keyaerts, J.; Edwards, H.; Maloney, A.; Delgado, J.; King, L.; Foley, A.; Lecomte, F.; Reuberson, J.; Meier, C.; Batchelor, M. Discovery of 4-azaindoles as novel inhibitors of c-Met kinase. *Bioorg. Med. Chem. Lett.* **2009**, *19*, 2780–2784.
- (59) Koolman, H.; Heinrich, T.; Bottcher, H.; Rautenberg, W.; Reggelin, M. Syntheses of novel 2,3-diaryl-substituted 5-cyano-4-azaindoles exhibiting c-Met inhibition activity. *Bioorg. Med. Chem. Lett.* **2009**, *19*, 1879–1882.